Cell propagation of Cholera Toxin CTA ADP-ribosylating factor by exosome mediated transfer.

Cristiana Zanetti[1], Angelo Gallina[2], Alessia Fabbri[3], Sofia Parisi[3], Angela Palermo[3], Katia Fecchi[3], Zaira Boussadia[3], Maria Carollo[4], Mario Falchi[5], Luca Pasquini[4], Maria Luisa Fiani[3,*] and Massimo Sargiacomo[3,*]

1 Department of Oncology and Molecular Medicine, Istituto Superiore di Sanità, Viale Regina Elena 299, 00161 Rome, Italy

2 Department of Neurosciences, Istituto Superiore di Sanità, Viale Regina Elena 299, 00161 Rome, Italy

3 National Center for Global Health, Istituto Superiore di Sanità, Viale Regina Elena 299, 00161 Rome, Italy

4 Core Facilities – Cytometry Unit, Istituto Superiore di Sanità, Viale Regina Elena 299, 00161 Rome, Italy

5 National AIDS Center, Istituto Superiore di Sanità, Viale Regina Elena 299, 00161 Rome, Italy

E-Mails: cristiana.zanetti@iss.it (C.Z.); gallinaangelo@yahoo.com (A.G.); alessia.fabbri@iss.it (A.F.); sofia.parisi91@gmail.com (S.P.); annica86@hotmail.it (A.P); katia.fecchi@iss.it (K.F.); zaira.boussadia@iss.it (Z.B.); maria.carollo@iss.it (M.C.); mario.falchi@iss.it (M.F.); luca.pasquini@iss.it (L.P.); maria.fiani@iss.it (M.L.F.); massimo.sargiacomo@iss.it (M.S.)

* Correspondence: maria.fiani@iss.it; massimo.sargiacomo@iss.it; Tel.: +39-06-4990-2518;

Running title: Cholera toxin spread via exosomes

Abstract: Here we first report, how cholera toxin (CT) A subunit (CTA), the bacterial enzyme moiety responsible of cell signaling alteration, can take over the exosomal pathway, spread extracellularly and be transmitted in a cell population. A first evidence for long-term transmission of CT toxic effect via extracellular vesicles was obtained in CHO cells. To follow CT intracellular route towards exosome secretion we adopted a strategy apt to convert multivesicular body (MVB) derived exosomes in traceable fluorescent vectors. CT treated Me665 cells, a human melanoma cell line highly expressing caveolin-1 (Cav-1) and GM1, were used to purify and characterize fluorescent

Peer-reviewed version available at Int. J. Mol. Sci. 2018, 19, 1521; doi:10.3390/ijms19051521

exosomes. Our results clearly show association of CT with exosomes together with typical exosomal markers and the HSP90 and PDI molecules, the required membrane translocation elements of CTA to the cytoplasm. Confocal microscopy proved direct CT containing fluorescent exo transfer into CHO cells coupled with the morphological cell change characteristic of CT action. Moreover, direct assessment of cAMP levels in Me665 cells treated with CT containing exo showed an efficient induction of cAMP increase comparable with CT alone. From our results, we can infer that CT can exploit exosome-mediated cell communication to target and extend its pathophysiological action throughout cell tissues.

Keywords: Cholera toxin, exosomes, endocytic pathway, Caveolin-1, GM1 ganglioside

---

1. Introduction

Despite being in the 21st century, cholera remains an epidemic or endemic disease in many parts of the world. It is mainly caused by few serogroups of the bacterial strain *Vibrio cholerae* that colonizes the small intestine with the subsequent production of the Cholera Toxin (CT) [1]. CT is made up of two major subunits, A and B [2] in that similar to other members of the AB5 family of toxins, that once secreted by bacteria in the microenvironment as holotoxin, enter host cells by hijacking endogenous trafficking pathways that culminate in the induction of toxicity through the achievement of their specific targets [3]. The A subunit (CTA) represents the enzymatic portion of the enterotoxin and is composed of a globular A1 domain (CTA1), which possesses the ADP-ribosylating activity, and the A2 domain (CTA2) that stabilizes, by noncovalent binding, the homo-pentameric B5 subunits (CTB). CTB subunits form a ring-like structure that bind exclusively to GM1 gangliosides, whose location in plasma membrane are typically concentrated in signaling organized centers known as lipid rafts and caveolae [4-6]. Localization of cholera toxin within caveolae has triggered the idea that these sites may constitute clathrin independent carriers. Although there is no real demonstration that CT enters cells specifically through the caveolae pathway, experimental evidences have shown that GM1 and Caveolin-1 (Cav-1) expression levels are selective factors of caveolae/raft-dependent endocytosis of cholera toxin en route to the Golgi complex [7].

Exosomes (exo) are vesicles 30–150 nm in size and are generated by inward budding of endosomal membranes otherwise called multivesicular bodies (MVB) which encloses multiple exosomes [8, 9]. An increasing number of molecules have been described to enter and to be delivered by exosomes suggesting a central role for these vesicles that move in and out of the cells, functioning as shuttles for the delivery of molecules cargo between different cells whose cargo may be used for monitoring

the metabolic state of the cell [10-12]. However, purification and fine analysis of exo populations remains a challenge [13, 14].

Few studies have already examined the involvement of exo in toxins trafficking. In the case of *Bacillus anthracis,* authors have shown that the lethal factor (LF) of Antrax lethal toxin, a major *B. anthracis* virulence factor, is translocated into the lumen of endosomal intraluminal vesicles (ILVs), persists in them for days and can be transmitted to neighboring cells [15]. Trichosanthin (TCS), a plant toxin, is incorporated into intraluminal vesicles of the MVB and is then secreted in association with exosomes upon fusion of the MVB with the plasma membrane [16]. In this paper, we provide evidences that part of CT molecules, once linked to GM1 on the plasma membrane, are sorted to MVB and are secreted as exosomes. To follow the MVB/exosome route we take advantage of a new methodology based on the fluorescent labelling of the phospholipid bilayer of exosomes [17] that enabled us to trace and quantify exosomes secretion. Furthermore, we show that CT containing exosomes are transferred to recipient cells and are able to induce morphological and functional changes typical of CT intoxication.

2. Results

2.1 Extracellular vesicles isolated from CHO and Me665 cells upon CT incubation comprise the AB5 subunits

We previously reported that Cav-1, a protein structurally related to caveolae formation, is highly expressed in human metastatic melanoma cell lines and is retrieved in isolated fractions of extracellular vesicles (EV) [18]. Since caveolae constitute renowned docking places for CTB binding to GM1, we hypothesized that Cav-1 and CT might share the same endocytic pathway that leads to EVs secretion. We first evaluated relative levels of GM1 and Cav-1 in Me665 melanoma cells and CHO cells. Figure 1A shows that both cell types expressed these molecules, with an increase in Me665 cells.

Preprints (www.preprints.org) | NOT PEER-REVIEWED | Posted: 12 April 2018 doi:10.20944/preprints201804.0158.v1

Peer-reviewed version available at Int. J. Mol. Sci. 2018, 19, 1521; doi:10.3390/ijms19051521

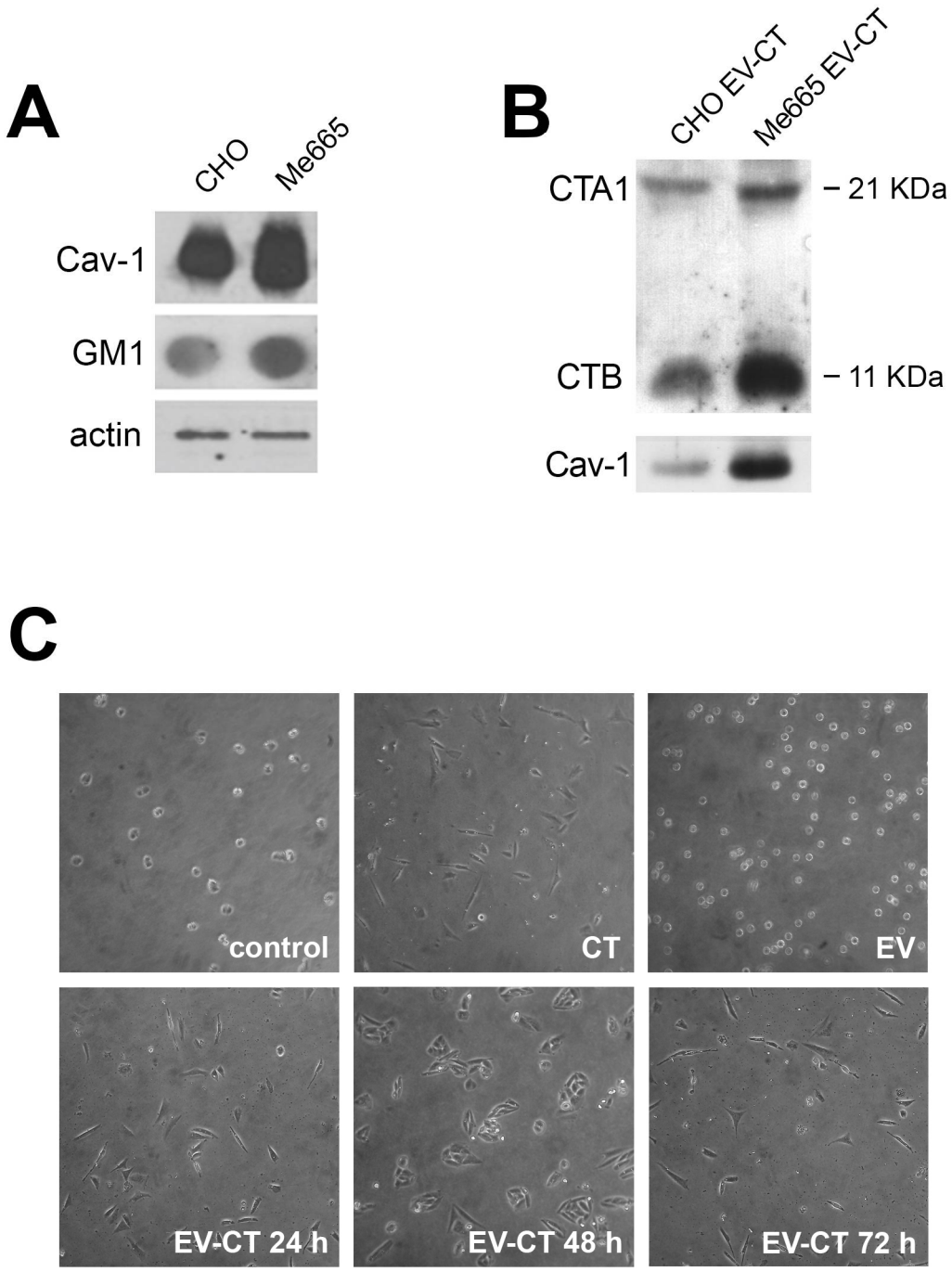

Figure 1. Expression of Cav-1 and GM1 in CHO and Me665 cells and morphological changes in CHO cells induced by CT-positive EVs (EV-CT) **(A)** Western blot analysis for Cav-1 and Dot blot analysis for GM1 of CHO and Me665 cell lines. For SDS-PAGE 30 µg of cell lysates were used and for Dot Blot 40 µg/dot. The presence of GM1 was assessed using horseradish peroxidase (HRP)-conjugated CTB. Actin is shown for normalization. **(B)** EVs collected from supernatants of CHO and

Peer-reviewed version available at Int. J. Mol. Sci. 2018, 19, 1521; doi:10.3390/ijms19051521

Me665 cells treated with CT were run on a SDS-PAGE gel in reducing conditions Western blot analysis with a polyclonal antibody for Cav-1 and CT is shown. **(C)** Light microscopy analysis of CHO cells upon addition of extracellular vesicles from control or CT treated CHO cells. EV were collected at different times from cell conditioned medium and isolated by differential ultracentrifugation. After isolation, EV were incubated for 6 h with CHO cells. 12 nM CT is used as positive control. At the end of the incubation, cells were analyzed with a light microscope.

To determine whether CT was secreted from cells as EVs, culture supernatants collected from the same number ($2x10^7$) of CT treated Me665 and CHO cells were subjected to differential centrifugations steps and vesicle pellets analyzed by western blot for CT presence. As shown in Figure 1B, CTA and CTB subunits were present in EV pellets from both cell types and were slightly more abundant in Me665 cells. Finally, to determine if CT carried by EVs was capable of inducing morphological changes in CHO cells as compared with CT we used a well-established CHO cell morphological assay [19]. For EVs purification, conditioned medium from cells treated or not with 12 nM CT for 2 h was collected at 24 h. After removal of conditioned medium, fresh medium was added twice for additional 24 h (EV-CT 48 h and EV-CT 72 h) and used for EVs purification. Figure 1C shows that 60-80% of freshly trypsinized CHO cells treated for 6 hours with EVs containing CT clearly became bipolar and elongated comparable to 12 nM CT alone. Most of the untreated cells were round even after overnight culture. Notably, EVs secreted after 48h or even 72 h from cells challenge with CT were also able to induce a morphological change indicating that functionally active CT is still transported by EVs.

2.2 Quantification and characterization of fluorescent exosomes containing CT demonstrate the CTA subunit inclusion.

Extracellular secretion gives rise to a variety of vesicles including those strictly derived from MVBs and properly defined exosomes. To better define the role of exo as carriers of toxins, among other types of EVs, we applied a method we have developed, based on the production of metabolically labelled fluorescent exo (F-exo) [17]. Accordingly, we labeled Me665 cells for 5 h with the phospholipid precursor BODIPY FL C16 (BODIPY C16) followed or not by the addition of 12 nM CT for 2 h and incubated for additional 24 h in fresh media. F-exo were purified by differential centrifugation from conditioned media and analyzed by FACS. As shown in Figure 2A both F-exo and F-exo CT appear as a discrete countable fluorescent population comparable for size and fluorescence intensity.

Preprints (www.preprints.org) | NOT PEER-REVIEWED | Posted: 12 April 2018 doi:10.20944/preprints201804.0158.v1

Peer-reviewed version available at Int. J. Mol. Sci. 2018, 19, 1521; doi:10.3390/ijms19051521

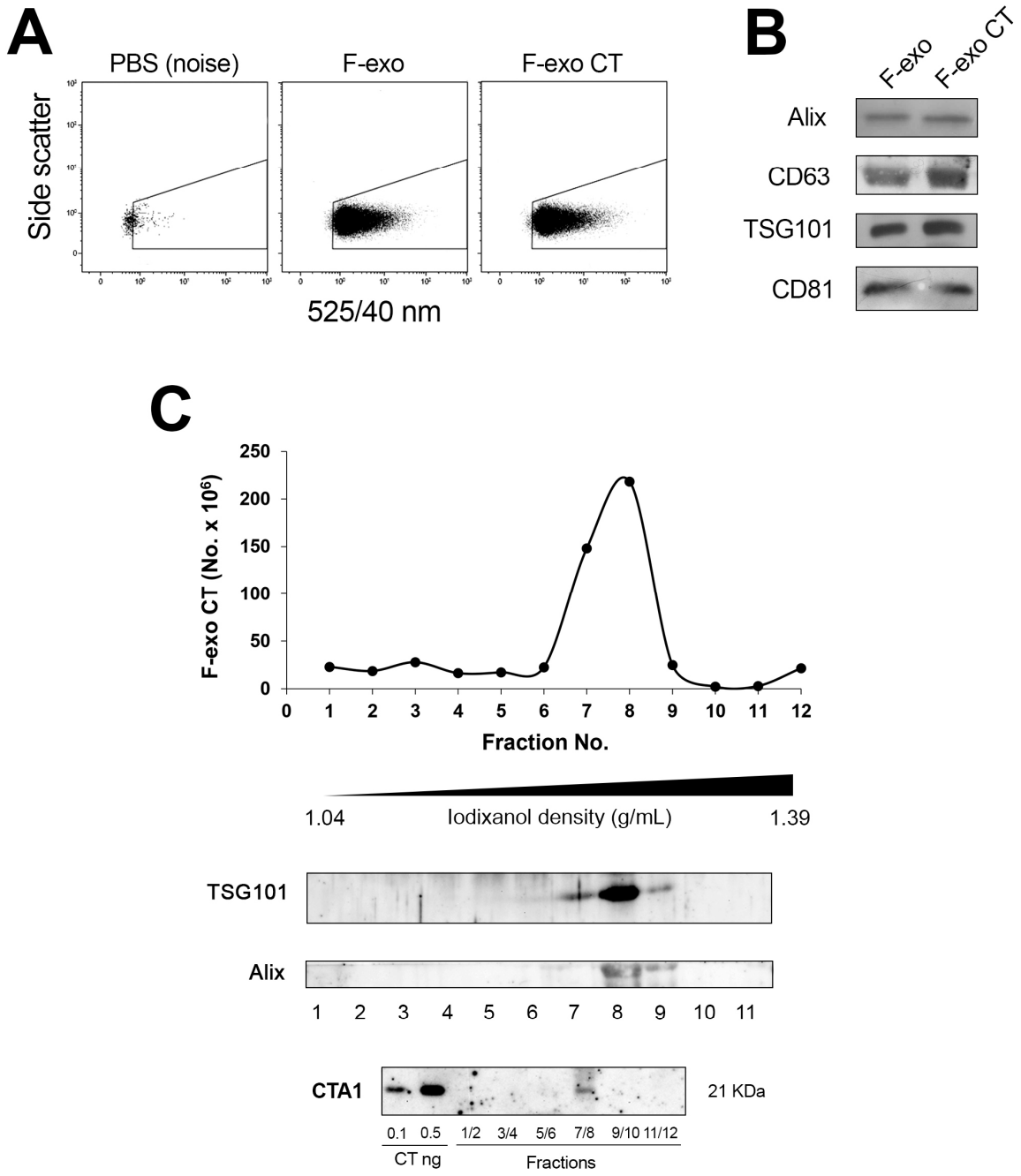

Figure 2. Characterization and distribution on iodixanol gradient of F-exo CT purified from Me665 cells. **(A)** FACS analysis of F-exo and F-exo CT deriving from Me665 cells incubated with or without 12 nM CT. To design the F-exo region above instrument background noise only PBS was acquired. Note that no events were registered in this region. **(B)** Western blot analysis of F-exo and F-exo CT probed with antibodies against exosome markers Alix, TSG101, CD63 and CD81. **(C)** The F-exo CT sample was loaded at the bottom of an iodixanol discontinuous density gradient and subjected to ultracentrifugation for 18 h. The resulting fractions (1-12) with increasing density were analyzed for vesicles number by FACS and for the presence of exosome markers TSG101 and ALIX

by Western blotting. The fluorescent peak displays a density ranging from 1.085 to 1.142. Fractions 1-2, 3-4, 5-6, 7-8, 9-10, 11-12 were pooled, TCA precipitated and analyzed by western blot after running a SDS-PAGE in reducing condition for the presence of CTA subunit. For Western blot, an equal volume of each sample was analyzed.

Same numbers of F-exo were characterized by Western blot analysis for the presence of typical exo markers as tetraspannins and ESCRT (endosomal-sorting complexes required for transport) components. Figure 2B shows that these markers are equally present in both F-exo and F-exo CT preparations thus showing that CT does not alter exosomal protein markers profile. To further characterize the F-exo population we loaded F-exo CT on top of a continuous iodixanol gradient to allow optimal separation of subtypes of EVs with different buoyant densities. The resulting fractions with increasing densities were analyzed for vesicles number by FACS (Figure 2C). F-exo CT separated in a discrete peak of density range 1.085-1.142 g/ml, as measured by refractometry, in accordance with the reported density of exosomes [8]. Western blot analysis of gradient fractions showed that exosomal markers TSG101 and Alix colocalized with the fluorescent peak fractions (fraction 7-8) thus further indicating that the F-exo population corresponds to bona fide exosomes. In order to assess the occurrence of CT active enzymatic moiety in F-exo we promptly subjected the pooled fractions 7-8 to immunoblot analysis with a monoclonal antibody against CTA. Results show that CTA1 was present in fractions corresponding to the F-exo fluorescent peak (Figure 2C).

2.3 Intracellular distribution of CT in Me665 cells

To visualize the intracellular localization and trafficking of CT, we first pulsed Me665 cells with BODIPY C16 for 5 h to metabolically label membrane sub-compartments. Successively cells were treated with 12 nM CT for 20 min on ice to allow binding to the plasma membrane. After CT incubation, cells were washed (T0) and fresh medium was added for further 24 h (T24). Following fixation, cells were analyzed by confocal microscopy. As shown in Figure 3A, at T0 CT clearly labeled only the plasma membrane and no colocalization with internal membrane compartments could be observed. Notably, lipid derived fluorescence was not present on the plasma membrane. After 24 h, CT was diffused in the cell cytoplasm as well as in discrete spots, presumably corresponding to late endosomal/MVB compartments, where it colocalized with lipid fluorescence.

Preprints (www.preprints.org) | NOT PEER-REVIEWED | Posted: 12 April 2018 doi:10.20944/preprints201804.0158.v1

Peer-reviewed version available at Int. J. Mol. Sci. 2018, 19, 1521; doi:10.3390/ijms19051521

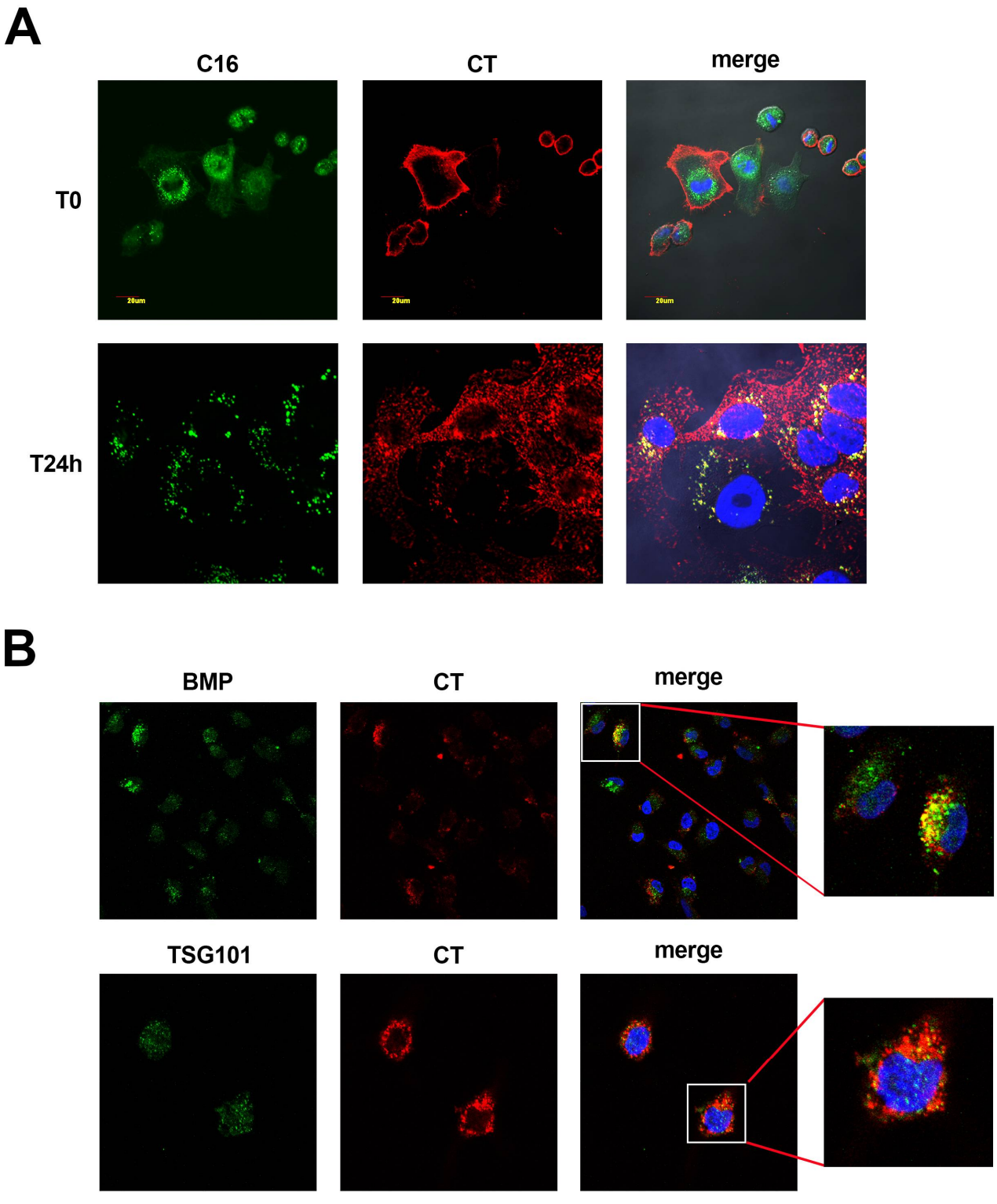

Figure 3. Intracellular distribution of CT in Me665 cells labelled with BODIPY C16

(A) Confocal microscopy analysis of Me665cells metabolically labelled with BODIPY C16, treated with 12 nM CT for 20 min on ice and then incubated with CT-free medium for 24 h at 37 °C. Images were taken at T0 and T24 h after the removal of CT. BODIPY C16 is represented in green and CT in red. **(B)** Cells, immunolabeled for BMP or TSG101 (green) and for CT (red) show colocalization of

Preprints (www.preprints.org) | NOT PEER-REVIEWED | Posted: 12 April 2018 doi:10.20944/preprints201804.0158.v1

Peer-reviewed version available at Int. J. Mol. Sci. 2018, 19, 1521; doi:10.3390/ijms19051521

both with CT, as evidenced in insets. Bar represents 20 µm. For all images DAPI staining was used for nuclear localization.

To better characterize the subcellular localization of CT we performed confocal microscopy analysis using antibodies against BMP, a lipid whose occurrence is specific of late endosomal MVB/lysosomal membrane tracking pathway [20], and TSG101, a component of ESCRT that functions in the early stage of MVB formation [21, 22]. Figure 3B shows that CT colocalized with both BMP and TSG101 (inset) providing additional proof of CT intersection with specific markers belonging to the exosomal trail.

2.4 CTA active subunit is retrieved in association HSP90/PDI with respect to F-exo biogenesis

With the aim of tracking F-exo CT biogenesis in Me665 cells, we pulsed cells with BODIPY C16 for 5 h in order to allow metabolic labeling of membrane compartments, including MVB. Cells were then chased in fresh media for 1 h, media was removed for exo purification and fresh media added up to 24 h to determine F-exo release time into the extracellular medium (Figure 4A).

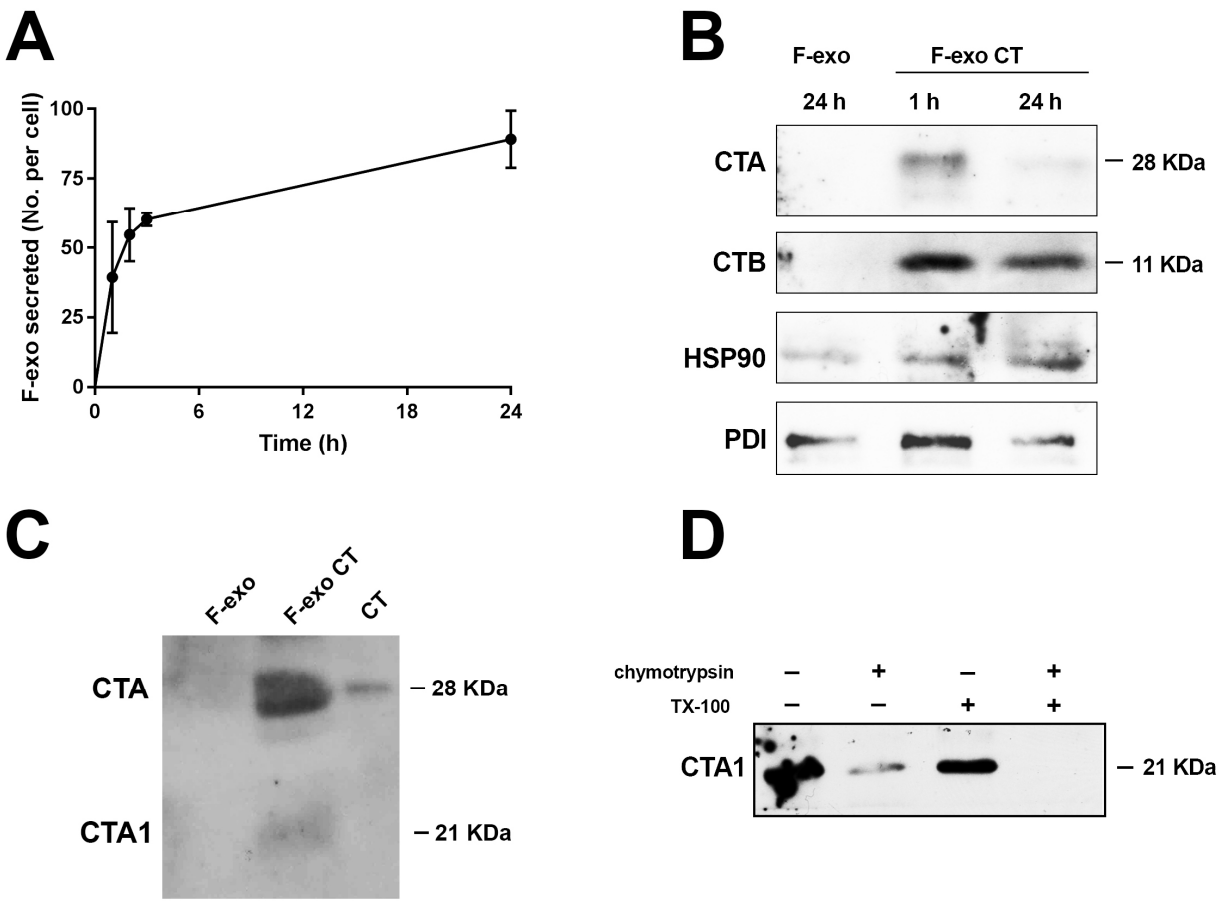

Figure 4. Exosome biogenesis and analysis of intra/extra localization of CT**. (A)** Me665 exosome biogenesis. Cells were pulsed with BODIPY C16 for 5 h for cell labelling, washed and complete

medium was added. Cell conditioned medium was harvested at different time points for exosome recovery and quantification by FACS. Amount of exo secreted per cell is shown. **(B)** Western Blot analysis of F-exo CT recovered at 1 h and 24 h subtracted of the 1h time point. The same number ($3x10^7$) of F-exo or F-exo CT were run on a non reducing SDS-PAGE gel, and immunoblotted for CTA and CTB subunits, HSP90 and PDI. **(C)** Western blot analysis of F-exo and F-exo CT ($6x10^7$) run in non-reducing conditions to show the presence of CTA1 and CTA1+CTA2 subunits. The monoclonal antibody anti-CTA reveal the presence of both the 28 kDa and the 21 kDa subunits. 0.3 ng of CT were used as positive control. **(D)** 16 µg of exo CT were incubated with 1 µg of chymotrypsin, in the absence or presence of 0.2 % Triton X-100. Samples were then loaded on SDS-PAGE gel in reducing conditions before western blot analysis using a monoclonal antibody anti-CTA.

Results show that as early as 1 h cells secrete a discrete population of F-exo that can be FACS counted. Equal numbers ($3x10^7$) of F-exo collected at 1 h and 24 h (subtracted of the 1 h time point sample) were run on SDS-PAGE and immunoblotted with antibodies against CTA and CTB subunits. In addition, the blots were probed for the presence of HSP90 and protein disulfide isomerase (PDI), proteins that have been shown to be specific requirements for membrane translocation from the ER to the cytosol of the unfolded CTA1 domain [23]. Figure 4B shows that CTA was present in F-exo throughout the exo biogenesis, and was more evident at early times (1 h) presumably because the cell CT reservoir was slowly decreasing over time. Interestingly, F-exo also contained the molecular chaperone HSP90 and PDI indicating that exo seem to constitute a cargo sharing system potentially able to spread toxicity all over the extracellular environment. Since PDI has the capability to dissociate the active CTA1 from the holotoxin, we therefore sought, by loading F-exo CT on a SDS-PAGE gel in non-reducing conditions, if the native 21 kDa CTA1 subunit was also present into vesicles. Figure 4C shows that both the 28 kDa CTA (CTA1+CTA2) and CTA1 bands resulted visible. Finally, to assess the localization of CTA, we exposed F-exo CT to chymotrypsin digestion with or without Triton X-100 assuming that CT molecules enclosed within exo lumen would be protected from hydrolysis (Figure 4D). Western blot analysis with an anti CTA monoclonal antibody showed that in absence of detergent chymotrypsin degraded a large part of CTA associated with exo while complete digestion could be obtained in presence of both chymotrypsin and Triton X-100. These results show that some portion of CTA, in that similar to the amount of the 21 kDa native subunit found in Figure 4C, is steadily present inside the vesicles because not reachable by chymotrypsin.

2.5 Functional activation of adenylate cyclase following F-exo direct transfer to cells

Preprints (www.preprints.org) | NOT PEER-REVIEWED | Posted: 12 April 2018 doi:10.20944/preprints201804.0158.v1

Peer-reviewed version available at Int. J. Mol. Sci. 2018, 19, 1521; doi:10.3390/ijms19051521

Exosomes play a central role in cell-to-cell communication by interaction with target cells. To induce a functional modification on the adenylate cyclase, therefore giving rise to increased levels of cAMP [24], exo containing CT must first be endocytosed by recipient cells. To determine the fate of F-exo we incubated CHO and Me665 with homologous F-exo containing or not CT. Transfer of F-exo was evaluated by confocal microscopy (Figure 5A).

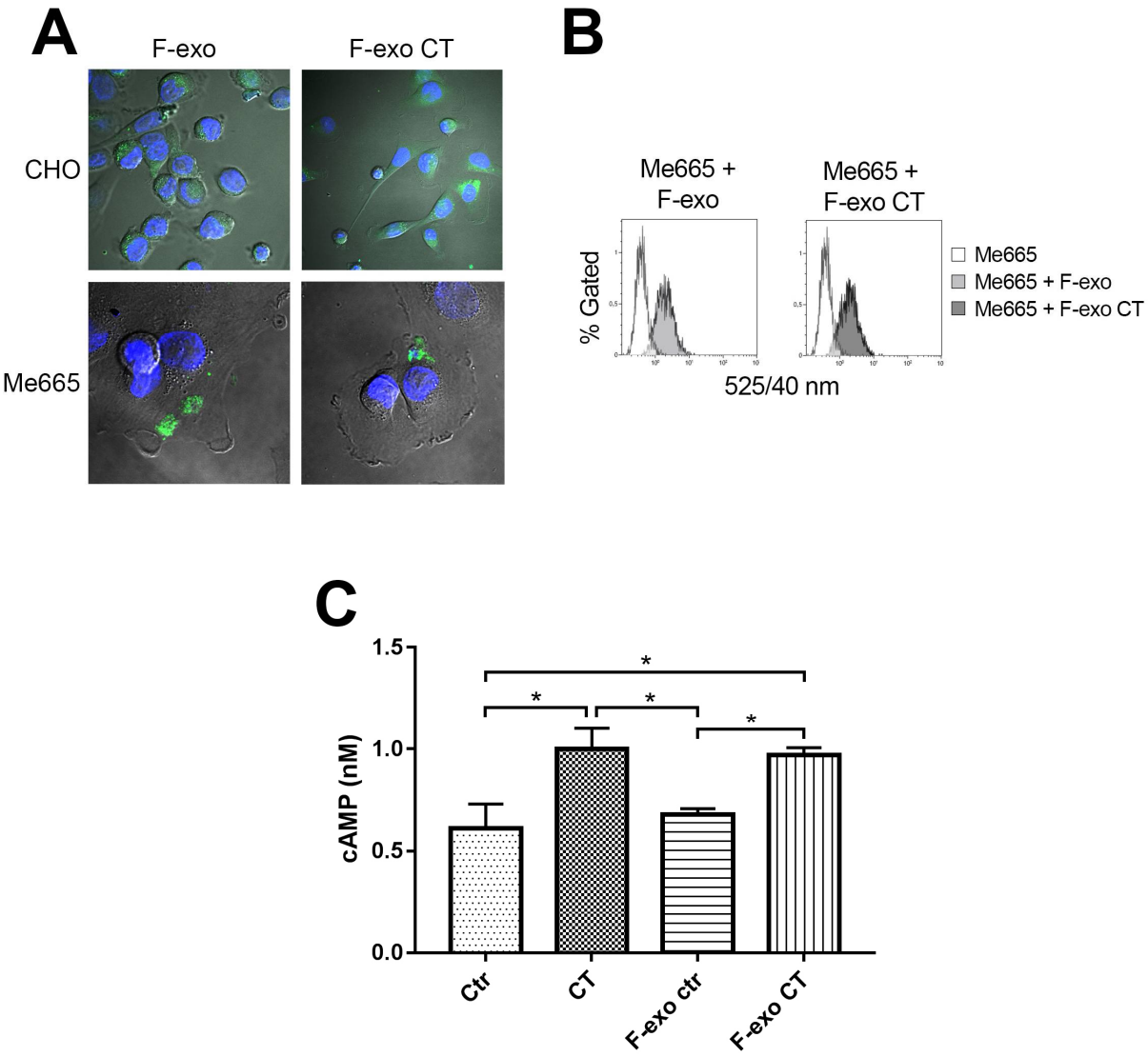

Figure 5. F-exo transfer to cells induces increase of cellular cAMP. **(A)** Confocal fluorescence microscopy images of F-exo and F-exo CT transfer on CHO and Me665 cells. $2x10^8$ fluorescent exosomes were incubated with $4x10^4$ CHO and Me665 cells for 4h at 37°C. Then cells were fixed and analysed. **(B)** FACS analysis of F-exo and F-exo CT transfer on target cells. $4x10^4$ cells were incubated with $1.5x10^7$ F-exo or F-exo CT for 4h at 37 °C. At the end of the incubation cells were FACS analysed. The increase in cell fluorescence demonstrate exosomes transfer to cells. **(C)** cAMP assay of Me665 cells treated with F-exo. $2x10^5$ cells were incubated with $5.7x10^7$ F-exo, F-exo CT

Preprints (www.preprints.org) | NOT PEER-REVIEWED | Posted: 12 April 2018 doi:10.20944/preprints201804.0158.v1

Peer-reviewed version available at Int. J. Mol. Sci. 2018, 19, 1521; doi:10.3390/ijms19051521

or 0.2 ng/ml CT for 4h at 37 °C. The graph shows the intracellular cAMP production of cells. * $p < 0.05$ Values are means ± S.D (n=3).

When CHO cells were treated with control F-exo no morphological changes were observed despite visible fluorescence uptake. In contrast, treatment with F-exo CT induced the characteristic elongated shape (Fig.5A upper panel). Transfer of F-exo could be observed also in Me665 cells, both by confocal microscopy (Fig.5A upper panel) or by direct assessment of fluorescence transfer by FACS analysis (Figure 5B). Finally, to assess directly functional activation of adenylate cyclase in Me665 cells, we treated cells with control F-exo, CT or F-exo CT for 4 h and measured cAMP levels by using a cAMP assay kit. CT (0.2 ng/ml) and F-exo CT had comparable effect and both increased cAMP level while control F-exo did not affect cellular cAMP thus demonstrating that CT carried by exosomes retains its biological activity.

3. Discussion

Cholera toxin cell entry and intracellular trafficking has been widely studied. There is a common consensus that GM1 based binding of CT is followed by retrograde vesicular trafficking from the plasma membrane through early endosomes, the Trans-Golgi, and the endoplasmic reticulum (ER), before the active CTA1 subunit reaches the cytosol and its final specific substrate [25]. These latter crucial steps appear to require interactions with host cell accessory proteins, as the chaperone Hsp90 and the protein-folding helper enzyme PDI, which make possible membrane translocation of the unfolded CTA1 domain [4, 26, 27]. Once in the cytosol CTA1 recovers the active conformation required for the ADP-ribosylation of its target, the α subunit of the heterotrimeric G protein (Gsα) [28, 29] that activates the adenylate cyclase, giving rise to increased levels of cellular cyclic AMP (cAMP) [30]. It is well known that CTB binding and cross-linking of five GM1 molecules serves to promote the function of lipid rafts in toxin trafficking, in fact lowering the expression of GM1 or cholesterol can prevent CT endocytosis [31-33]. However, how GM1 undertakes a specific lipid trafficking route has not been completely assessed. Despite many aspects of CT-GM1 retrograde trafficking from PM to ER have been elucidated, when all the three CT major pathways of entry, i.e. caveolin, clathrin, or Arf6 dependent, are inhibited no significant reduction of toxicity was observed whereby one or more unknown pathways have been hypothesized [34]. Moreover, a retracing study of CT intoxicating retrograde pathways carried out using a subset of GM1 specified by saturated or unsaturated fluorescent-labeled ceramide chains showed that CT bound to saturated GM1, differently from the unsaturated complex forms, are directed towards late endosome compartments (that includes the MVB containing exosomes) rather than the classical Golgi/ER pathway [35]. Accordingly, it has

been reported that GM1 gangliosides localize in the membrane of exosomes [36]. Notably previous studies showed that caveolae and lipid raft associated proteins and lipids can take part in cell-derived exosomes (exo) secretion [18, 37, 38]. In this study, we reported for the first time that CT can be propagated via EVs in a biologically active form and that CT persist in cells long after treatment with the toxin. Accordingly vesicles collected up to 72h, still contain biologically active CT. Cells release different types of microvesicles, not all of endo/lysosomal origin like ectosomes that directly bud from the plasma membrane [20]. To distinguish among different types of vesicles we applied a novel methodology for the metabolic labelling of exo that we developed in our lab [17]. BODIPY C16, a fluorescent phospholipid precursor, is efficiently incorporated into cells and once is metabolized in the ER takes the endosomal/MVB route to become integral part of the exosome membrane. Fluorescent exo are then secreted in the extracellular medium and can be purified and counted. We show here that CTA is associated with a discrete population of fluorescent exo that express typical exo markers (Figure 2). Furthermore, this methodology consented us to highlight intracellular membranes compartments that intersect CT journey (Figure 3A) specifically in the endolysosomal compartment as shown by colocalization of CT with MVBs specific markers (Figure 3B). This finding suggests that exosomes, in addition of being a mean of transport, may represent a kind of CT-repository within the MVBs, allowing CT to be protected from intracellular degradation and allowing for long-term activity. F-exo biogenesis studies consented us to monitor CT secretion over time highlighting an early release at 1 h of F-exo containing CT. At later times (24 h) CT was still present in F-exo but in lower amounts showing that, the bulk of CT associated with exo is released at the initial stages after toxin binding. Interestingly, the host cell chaperone HSP90, an established exosomal marker [39], and protein-helper enzyme PDI were both clearly present throughout the exo biogenesis together with CT subunits (Figure 4B). Furthermore, CTA was present in exo both in the active reduced form, CTA1 (21 kDa) or as the disulfide linked CTA1 and CTA2 (28 kDa) form. Chymotrypsin digestion of F-exo containing CT revealed that the CTA subunit is distributed both outside and inside of exosomes. Based on our results an appealing speculation is that CTA associated with exo may derive from two distinct intracellular routes. One envisage that upon cell entry part of CT molecules may follow the long chain saturated GM1 pathway [35] presumably along with Cav-1, that leads to the CT holotoxin direct sorting to the late endosomal compartment/MVB before being secreted. The other, namely CTA1, is originated from the canonical ER retrograde pathway where, by the action of HSP90 and PDI, is translocated to the cytosol and taken up during exo formation by intraluminal vesicles.

Peer-reviewed version available at Int. J. Mol. Sci. 2018, 19, 1521; doi:10.3390/ijms19051521

In final experiments F-exo were used to demonstrate the strict relation between the cellular uptake of CT containing exo that in CHO cells was highlighted by the morphological changes and in Me665 by direct increase of cellular cAMP levels.

In conclusion, starting from the more general hypothesis, which assumes that exosomes are vehicles that rule cell homeostasis, we found that CT could exploit the exosomal pathway to amplify its action from a single cell to an entire cell population. This study suggests an important role for exosomes in cholera pathogenesis and on the dynamic of infectious disease given that these native vehicles seem to preserve, protect and transfer the toxin from cell to cell.

4. Materials and Methods

4.1 Cell culture

The Human melanoma cell line, Me665/1 (Me665), stabilized from surgical specimen obtained from metastatic lesions at Istituto Nazionale Tumori (Milan, Italy) and CHO (Chinese hamster ovary) cell line commercially available, were grown in Dulbecco's modified Eagle's medium (DMEM) (EuroClone) supplemented with 10% fetal bovine serum (Biological Industries), 5 mM L-glutamine, penicillin (100 units/ml) and streptomycin (100 µg/ml) at 37°C in a humidified 5% CO_2 atmosphere.

4.2 Isolation of EVs from CHO and Me665 cell culture supernatants

For isolation of EVs, subconfluent monolayers of CHO and Me665 cells in exponential growth were incubated in DMEM supplemented with 0.3 % FBS with or without 12 nM CT, purified from culture filtrates of *Vibrio Cholerae* 569 B, serotype Inaba as described by [40]. After 2 h of CT treatment, control and treated cells were washed in PBS and further cultured in fresh DMEM medium for 24 h before collection of medium for EVs isolation. EVs were isolated from the culture supernatants of treated and untreated cells by sequential centrifugations as previously described [17, 41] with some modifications. Briefly, culture supernatant was centrifuged at 2,000 x *g* for 20 min at 4°C to pellet cells debris. Supernatants were transferred to new tubes and centrifuged in a SW41Ti rotor (Beckman) at 10,000 x *g* for 20 min at 4 °C, and finally ultracentrifuged at 100,000 x *g* for 3 h. Pellets were washed in PBS and ultracentrifuged at the same speed for 3 h.

4.3 Morphological analysis of CHO cells after CT, EV and EV-CT treatment

Exponentially growing CHO cells were harvested and transferred to 12-well plates ($2x10^4$ cells/well). DMEM supplemented with 0.3 % FCS was added with or without 12 nM CT, with EV and EV-CT

Preprints (www.preprints.org) | NOT PEER-REVIEWED | Posted: 12 April 2018 doi:10.20944/preprints201804.0158.v1

Peer-reviewed version available at Int. J. Mol. Sci. 2018, 19, 1521; doi:10.3390/ijms19051521

(prepared as described above). After 6 h incubation, cells were inspected microscopically to analyze the morphological changes.

4.4 Dot blot and Western blot analysis

Cell pellets were lysed in 20 mM Tris, pH 7.4, 150 mM NaCl, 1% Triton X-100, 2 mM EDTA with a Protease Inhibitor Cocktail (Roche) for 20 min on ice and then centrifuged at 2,000 x g for 10 min. Pellet was discarded and supernatant was kept for further analysis. Protein concentration was measured using the BCA assay (Thermo Scientific). The presence of GM1 ganglioside in cell lysates was assessed by dot blot assay using horseradish peroxidase (HRP)-conjugated CTB subunit and revealed with an ECL detection kit (Pierce). Cell lysates (40 µg), were boiled and spotted onto a nitrocellulose membrane blocked using 5% Blotting Grade non-fat dry milk in TBS-Tween (TBST) buffer (10 mM Tris-HCl (pH 8.0), 150 mM NaCl, 0.1% Tween 20) for 45 min at room temperature (RT) followed by incubation with HRP-CTB dissolved in TBST buffer (1:400) for 1 h at RT. The reactivity was detected using an ECL detection kit (Pierce). For Western Blot analysis, exosome preparations were lysed in Laemmli sample buffer, boiled and loaded on 10 or 14% SDS-PAGE gel under reducing or non-reducing conditions. Proteins were blotted onto a nitrocellulose membrane, blocked using 5% Blotting Grade non-fat dry milk in TBS-Tween (TBST) buffer (10 mM Tris-HCl (pH 8.0), 150 mM NaCl, 0.1% Tween 20) for 1 h at RT followed by incubation with primary antibodies. The following primary antibodies were used: mouse anti-Cholera Toxin A (Clone 2H9) (Immunology Consultants Laboratory, Inc.) 1:500 and rabbit polyclonal Anti-Cholera toxin (Sigma-Aldrich) 1:1000; rabbit anti-Caveolin-1 (N-20) (Santa Cruz Biotechnology) 1:1000; rabbit anti-Protein Disulfide Isomerase Polyclonal Antibody (StressGen) 1:1000; rabbit anti-HSP90 α/β (H-114) (Santa Cruz Biotechnology) 1:1000 dissolved in TBS-Tween (TBST) buffer for 1h at RT; mouse anti-Alix (3A9) (Thermo scientific) 1:1000, rabbit anti-CD63 (SBI) 1:1000, mouse anti-CD81 1:1000, mouse anti-TSG101 (GeneTex) 1:1000 dissolved in 0,25% Blotting Grade non-fat dry milk in TBST overnight at 4°C. After washing with TBST, filters were incubated with appropriate horseradish peroxidase-conjugated secondary antibodies (Bio-Rad) for 1 h at RT, and immunoreactivity was revealed by using an ECL detection kit (Pierce).

4.5 Generation and quantification of F-exo

F-exo were purified and quantified as previously described [17]. Briefly, melanoma cells Me665 ($8x10^5$) were incubated with 7 µM BODIPY FL C_{16} (4,4-difluoro-5,7-dimethyl-4-bora-3a,4a-diaza-s-indacene-3-hexadecanoic acid) (BODIPY C16) (Life Technologies) for 5 h at 37 °C in DMEM supplemented 0.3% FCS and then excess probe was removed by washing in PBS. Subsequently, cells

Preprints (www.preprints.org) | NOT PEER-REVIEWED | Posted: 12 April 2018 doi:10.20944/preprints201804.0158.v1

Peer-reviewed version available at Int. J. Mol. Sci. 2018, 19, 1521; doi:10.3390/ijms19051521

were incubated with or without 12 nM CT for 2 h at 37°C and then washed with PBS to remove the excess of CT. F-exo and F-exo CT purification was performed as previously described by differential ultracentrifugations. The resulting pellet was quantified by FACS (FC Gallios Flow Cytometer and Kaluza Software - Beckman Coulter). To set the instrument, fluorescent beads (525/540 nm FL1) ranging in size from 0.1 to 0.5 µm were analyzed. Flow count fluorospheres, used to determine exo number, were resuspended in PBS with F-exo and F-exo CT and the instrument was set to fix the stopping gate on 2,000 flow count fluorospheres. For further details refer to [17]. For F-exo biogenesis studies, F-exo CT were collected at different time points (1 h-24 h) after 2 h CT incubation.

4.6 Iodixanol/OptiPrep™ gradient separation

A discontinuous iodixanol gradient was used for further exosome purification, as described by several authors [42]. Solutions of 10 %, 30 % and 40 % iodixanol were made up by mixing appropriate amounts of homogenization buffer (HM solution: 0.25M sucrose, 1 mM EDTA, 10 mM Tris-HCL pH=7,4) and an iodixanol working solution. This working solution was prepared by combining a working solution buffer (0.25 M sucrose, 6mM EDTA, 60 mM Tris-HCL pH=7,4) and a stock solution of OptiPrep™ (60% w/v aqueous iodixanol solution). The gradient was formed by layering 1ml of 60% with 0.260 ml sample, 0.5 ml 40%, 0.5 ml 30% and 1.8 ml of 10% solutions on top in a 4.5 ml open top polyallomer tube (Beckman Coulter). The gradient was then centrifuged for 18 h at 192,000 x *g* at 4 °C (SW60 Ti rotor Beckman Coulter). Gradient fractions of 350 µl were collected from the top of the gradient and analyzed by FACS for exosome count. Fractions were loaded on a SDS-PAGE gel for Western blotting analysis, using antibodies directed against exosome markers TSG101 and Alix. For CT detection, gradient fractions were TCA precipitated. Refractive index of each fraction was assessed with a refractometer (Carl Zeiss) and the relative density was calculated using the linear relationship between refractive index (η) and the density (ρ) $\rho = A\eta - B$.

4.7 Chymotrypsin treatment of exo

To analyze the intra/extra localization of CT, exo CT (16 µg) were incubated with 1µg of chymotrypsin, in the absence or presence of 0.2% Triton X-100, at 37 °C for 3 hour at pH 7.8. Digestion was stopped on ice with 5 µM phenylmethanesulfonyl fluoride (PMSF). Samples were then mixed with Laemmli buffer, heated at 95 °C for 5 min, and analyzed by SDS-PAGE and western blotting.

4.8 cAMP Assay

Preprints (www.preprints.org) | NOT PEER-REVIEWED | Posted: 12 April 2018 doi:10.20944/preprints201804.0158.v1

Peer-reviewed version available at Int. J. Mol. Sci. 2018, 19, 1521; doi:10.3390/ijms19051521

Freshly trypsinized cells were transferred to 6-well plates ($2x10^5$ cells/well) and incubated overnight at 37 °C in DMEM with 10% FCS to allow cell attachment. Plates were then washed with serum-free DMEM, and 1 ml of 1% FCS DMEM containing 0.5 mM 1-methyl-3-isobutylxantine (IBMX, Sigma) was added for 30 min. As control IBMX treated cells were used. After incubation, 0.2 ng/ml of CT or a specific number ($5.7x10^7$) of F-exo and F-exo CT were added and plates were incubated at 37 °C for 4 h. Cells were washed in ice-cold PBS and cAMP assay was performed according to manufacturer's instructions (Cyclic AMP XP Assay kit, Cell Signaling).

4.9 Confocal Microscopy

To analyze the intracellular colocalization of CT with exo, Me665cells ($4x10^4$) were cultured on 24-well plates containing coverslips until 60-70% of confluency. Cells were incubated at 37 °C with or without 7 µM BODIPY C16 for 4 h. 12 nM CT was added for 20 min on ice (T0), and cells were then incubated at 37 °C for 24 h (T24). Cells were fixed with 3 % paraformaldehyde (PFA) for 20 min at RT and permeabilized with 0.05% saponin. Primary antibodies used were: rabbit polyclonal anti-Cholera toxin (Sigma-Aldrich), mouse anti-TSG101 (GeneTex), mouse anti-LBPA/BMP (6C4) (Echelon). AlexaFluor647-conjugated and AlexaFluor488-conjugated goat anti mouse or anti rabbit (Life Technologies) was used as secondary antibody. Coverslips were mounted on the microscope slide with Vectashield antifade mounting medium containing DAPI (Vector Laboratories, Burlingame, CA). Images were taken by a FV1000 confocal microscope (Olympus, Tokyo, Japan), using a (Olympus) planapo objective 60x oil A.N. 1.42. Excitation light was obtained by a Laser Dapi 408 nm for DAPI, an Argon Ion Laser (488 nm) for FITC (Alexa 488), and a Red Diode Laser (638 nm) for Alexa 647. DAPI emission was recorded from 415 to 485 nm, FITC emission was recorded from 495 to 550 nm, and Alexa 647 from 634 to 750 nm. Images recorded have an optical thickness of 0.3 mm.

4.10 F-exo and F-exo CT transfer

To evaluate the transfer on target cells, F-exo were incubated with cells in a 24-well plate in duplicate in 1 ml DMEM with 0.1% FCS and kept for 4 h at 37 °C in CO_2 incubator. Medium was then removed and cells PBS washed, detached and subjected to FACS analysis for cell fluorescence. For confocal microscopy $4x10^4$ cells were seeded on a sterilized coverslip and incubated with $2x10^8$ F-exo or F-exo CT for 4 h at 37 °C in DMEM with 0.1 % FCS. At the end of incubation, medium was removed, cells were PBS washed and fixed with 3% PFA for the analysis.

Acknowledgments

This work was supported by a grant from "Ricerca Finalizzata" project n. 2011-02347300 from the Ministry of Health, Italy to M.S. We also gratefully thank Tommaso Costa for helpful discussions and valuable advice.

Author Contributions

Cristiana Zanetti, Angelo Gallina and Alessia Fabbri performed the experiments and analyzed the data; Sofia Parisi, Angela Palermo, Katia Fecchi, Zaira Boussadia, Maria Carollo, Mario Falchi and Luca Pasquini, performed the experiments; Cristiana Zanetti, Maria Luisa Fiani and Massimo Sargiacomo wrote the paper; Maria Luisa Fiani and Massimo Sargiacomo conceived and designed the experiments and analyzed the data.

Conflicts of Interest

The authors declare no conflict of interest.

References

1. Chatterjee, D.; Chaudhuri, K., Association of cholera toxin withVibrio choleraeouter membrane vesicles which are internalized by human intestinal epithelial cells. *FEBS letters* **2011,** 585, (9), 1357-1362.
2. Gill, D. M.; Rappaport, R. S., Origin of the Enzymatically Active AI Fragment of Cholera Toxin. *Journal of Infectious Diseases* **1979,** 139, (6), 674-680.
3. Sandvig, K.; Deurs, B. v., Transport of protein toxins into cells: pathways used by ricin, cholera toxin and Shiga toxin. *FEBS letters* **2002,** 529, (1), 49-53.
4. Sánchez, J.; Holmgren, J., Cholera toxin structure, gene regulation and pathophysiological and immunological aspects. *Cellular and Molecular Life Sciences* **2008,** 65, (9), 1347-1360.
5. Parton, R. G., Ultrastructural localization of gangliosides; GM1 is concentrated in caveolae. *Journal of Histochemistry & Cytochemistry* **1994,** 42, (2), 155-166.
6. Taylor, M.; Banerjee, T.; Navarro-Garcia, F.; Huerta, J.; Massey, S.; Burlingame, M.; Pande, A. H.; Tatulian, S. A.; Teter, K., A therapeutic chemical chaperone inhibits cholera intoxication and unfolding/translocation of the cholera toxin A1 subunit. *PloS one* **2011,** 6, (4), e18825.
7. Pang, H.; Le, P. U.; Nabi, I. R., Ganglioside GM1 levels are a determinant of the extent of caveolae/raft-dependent endocytosis of cholera toxin to the Golgi apparatus. *Journal of cell science* **2004,** 117, (8), 1421.
8. Colombo, M.; Raposo, G.; Théry, C., Biogenesis, Secretion, and Intercellular Interactions of Exosomes and Other Extracellular Vesicles. *Annual Review of Cell and Developmental Biology* **2014,** 30, (1), 255-289.
9. Lo Cicero, A.; Stahl, P. D.; Raposo, G., Extracellular vesicles shuffling intercellular messages: for good or for bad. *Current opinion in cell biology* **2015,** 35, 69-77.
10. El Andaloussi, S.; Lakhal, S.; Mäger, I.; Wood, M. J. A., Exosomes for targeted siRNA delivery across biological barriers. *Advanced Drug Delivery Reviews* **2013,** 65, (3), 391-397.

11. Mathivanan, S.; Ji, H.; Simpson, R. J., Exosomes: extracellular organelles important in intercellular communication. *J Proteomics* **2010,** 73, (10), 1907-20.
12. Simons, M.; Raposo, G., Exosomes--vesicular carriers for intercellular communication. *Current opinion in cell biology* **2009,** 21, (4), 575-81.
13. Yang, F.; Liao, X.; Tian, Y.; Li, G., Exosome separation using microfluidic systems: size‐based, immunoaffinity‐based and dynamic methodologies. *Biotechnology Journal* **2017,** 12, (4), 1600699.
14. Zavec Apolonija, B.; Kralj‐Iglič, V.; Brinc, M.; Trček Tanja, F.; Kuzman, D.; Schweiger, A.; Anderluh, G., Extracellular vesicles concentration is a promising and important parameter for industrial bioprocess monitoring. *Biotechnology Journal* **2016,** 11, (5), 603-609.
15. Abrami, L.; Brandi, L.; Moayeri, M.; Brown, M. J.; Krantz, B. A.; Leppla, S. H.; van der Goot, F. G., Hijacking multivesicular bodies enables long-term and exosome-mediated long-distance action of anthrax toxin. *Cell reports* **2013,** 5, (4), 986-96.
16. Zhang, F.; Sun, S.; Feng, D.; Zhao, W. L.; Sui, S. F., A novel strategy for the invasive toxin: hijacking exosome-mediated intercellular trafficking. *Traffic* **2009,** 10, (4), 411-24.
17. Coscia, C.; Parolini, I.; Sanchez, M.; Biffoni, M.; Boussadia, Z.; Zanetti, C.; Fiani, M. L.; Sargiacomo, M., Generation, Quantification, and Tracing of Metabolically Labeled Fluorescent Exosomes. In *Lentiviral Vectors and Exosomes as Gene and Protein Delivery Tools*, Federico, M., Ed. Springer New York: New York, NY, 2016; pp 217-235.
18. Felicetti, F.; Parolini, I.; Bottero, L.; Fecchi, K.; Errico, M. C.; Raggi, C.; Biffoni, M.; Spadaro, F.; Lisanti, M. P.; Sargiacomo, M.; Care, A., Caveolin-1 tumor-promoting role in human melanoma. *International journal of cancer. Journal international du cancer* **2009,** 125, (7), 1514-22.
19. Morinaga, N.; Kaihou, Y.; Vitale, N.; Moss, J.; Noda, M., Involvement of ADP-ribosylation Factor 1 in Cholera Toxin-induced Morphological Changes of Chinese Hamster Ovary Cells. *Journal of Biological Chemistry* **2001,** 276, (25), 22838-22843.
20. Record, M.; Carayon, K.; Poirot, M.; Silvente-Poirot, S., Exosomes as new vesicular lipid transporters involved in cell-cell communication and various pathophysiologies. *Biochimica et biophysica acta* **2014,** 1841, (1), 108-20.
21. Tan, S. S.; Yin, Y.; Lee, T.; Lai, R. C.; Yeo, R. W.; Zhang, B.; Choo, A.; Lim, S. K., Therapeutic MSC exosomes are derived from lipid raft microdomains in the plasma membrane. *J Extracell Vesicles* **2013,** 2.
22. Lotvall, J.; Hill, A. F.; Hochberg, F.; Buzas, E. I.; Di Vizio, D.; Gardiner, C.; Gho, Y. S.; Kurochkin, I. V.; Mathivanan, S.; Quesenberry, P.; Sahoo, S.; Tahara, H.; Wauben, M. H.; Witwer, K. W.; Thery, C., Minimal experimental requirements for definition of extracellular vesicles and their functions: a position statement from the International Society for Extracellular Vesicles. *J Extracell Vesicles* **2014,** 3, 26913.
23. Ernst, K.; Schnell, L.; Barth, H., Host Cell Chaperones Hsp70/Hsp90 and Peptidyl-Prolyl Cis/Trans Isomerases Are Required for the Membrane Translocation of Bacterial ADP-Ribosylating Toxins. *Current topics in microbiology and immunology* **2017,** 406, 163-198.
24. Guerrant, R. L.; Brunton, L. L.; Schnaitman, T. C.; Rebhun, L. I.; Gilman, A. G., Cyclic adenosine monophosphate and alteration of Chinese hamster ovary cell morphology: a rapid, sensitive in vitro assay for the enterotoxins of Vibrio cholerae and Escherichia coli. *Infection and immunity* **1974,** 10, (2), 320-7.
25. Wernick, N. L. B.; Chinnapen, D. J. F.; Cho, J. A.; Lencer, W. I., Cholera Toxin: An Intracellular Journey into the Cytosol by Way of the Endoplasmic Reticulum. *Toxins* **2010,** 2, (3), 310-325.

26. Taylor, M.; Burress, H.; Banerjee, T.; Ray, S.; Curtis, D.; Tatulian, S. A.; Teter, K., Substrate-induced unfolding of protein disulfide isomerase displaces the cholera toxin A1 subunit from its holotoxin. *PLoS pathogens* **2014,** 10, (2), e1003925.
27. Taylor, M.; Navarro-Garcia, F.; Huerta, J.; Burress, H.; Massey, S.; Ireton, K.; Teter, K., Hsp90 Is Required for Transfer of the Cholera Toxin A1 Subunit from the Endoplasmic Reticulum to the Cytosol. *The Journal of biological chemistry* **2010,** 285, (41), 31261-31267.
28. Pande, A. H.; Scaglione, P.; Taylor, M.; Nemec, K. N.; Tuthill, S.; Moe, D.; Holmes, R. K.; Tatulian, S. A.; Teter, K., Conformational instability of the cholera toxin A1 polypeptide. *Journal of molecular biology* **2007,** 374, (4), 1114-28.
29. Ampapathi, R. S.; Creath, A. L.; Lou, D. I.; Craft, J. W., Jr.; Blanke, S. R.; Legge, G. B., Order-disorder-order transitions mediate the activation of cholera toxin. *Journal of molecular biology* **2008,** 377, (3), 748-60.
30. Kaper, J. B.; Morris, J. G.; Levine, M. M., Cholera. *Clinical microbiology reviews* **1995,** 8, (1), 48-86.
31. Lencer, W. I.; Tsai, B., The intracellular voyage of cholera toxin: going retro. *Trends in biochemical sciences* **2003,** 28, (12), 639-45.
32. Saslowsky, D. E.; Lencer, W. I., Conversion of apical plasma membrane sphingomyelin to ceramide attenuates the intoxication of host cells by cholera toxin. *Cellular microbiology* **2008,** 10, (1), 67-80.
33. Wolf, A. A.; Fujinaga, Y.; Lencer, W. I., Uncoupling of the cholera toxin-G(M1) ganglioside receptor complex from endocytosis, retrograde Golgi trafficking, and downstream signal transduction by depletion of membrane cholesterol. *The Journal of biological chemistry* **2002,** 277, (18), 16249-56.
34. Massol, R. H.; Larsen, J. E.; Fujinaga, Y.; Lencer, W. I.; Kirchhausen, T., Cholera toxin toxicity does not require functional Arf6- and dynamin-dependent endocytic pathways. *Molecular biology of the cell* **2004,** 15, (8), 3631-41.
35. Chinnapen, D. J.; Hsieh, W. T.; te Welscher, Y. M.; Saslowsky, D. E.; Kaoutzani, L.; Brandsma, E.; D'Auria, L.; Park, H.; Wagner, J. S.; Drake, K. R.; Kang, M.; Benjamin, T.; Ullman, M. D.; Costello, C. E.; Kenworthy, A. K.; Baumgart, T.; Massol, R. H.; Lencer, W. I., Lipid sorting by ceramide structure from plasma membrane to ER for the cholera toxin receptor ganglioside GM1. *Developmental cell* **2012,** 23, (3), 573-86.
36. de Gassart, A.; Géminard, C.; Février, B.; Raposo, G.; Vidal, M., Lipid raft-associated protein sorting in exosomes. *Blood* **2003,** 102, (13), 4336.
37. Calzolari, A.; Raggi, C.; Deaglio, S.; Sposi, N. M.; Stafsnes, M.; Fecchi, K.; Parolini, I.; Malavasi, F.; Peschle, C.; Sargiacomo, M.; Testa, U., TfR2 localizes in lipid raft domains and is released in exosomes to activate signal transduction along the MAPK pathway. *Journal of cell science* **2006,** 119, (Pt 21), 4486-98.
38. Parolini, I.; Federici, C.; Raggi, C.; Lugini, L.; Palleschi, S.; De Milito, A.; Coscia, C.; Iessi, E.; Logozzi, M.; Molinari, A.; Colone, M.; Tatti, M.; Sargiacomo, M.; Fais, S., Microenvironmental pH is a key factor for exosome traffic in tumor cells. *The Journal of biological chemistry* **2009,** 284, (49), 34211-22.
39. Kowal, J.; Arras, G.; Colombo, M.; Jouve, M.; Morath, J. P.; Primdal-Bengtson, B.; Dingli, F.; Loew, D.; Tkach, M.; Théry, C., Proteomic comparison defines novel markers to characterize heterogeneous populations of extracellular vesicle subtypes. *Proceedings of the National Academy of Sciences* **2016,** 113, (8), E968-E977.
40. Tomasi, M.; Battistini, A.; Araco, A.; Roda, L. G.; D'Agnolo, G., The Role of the Reactive Disulfide Bond in the Interaction of Cholera-Toxin Functional Regions. *European journal of biochemistry* **1979,** 93, (3), 621-627.

41. Thery, C.; Amigorena, S.; Raposo, G.; Clayton, A., Isolation and characterization of exosomes from cell culture supernatants and biological fluids. In *Current protocols in cell biology / editorial board, Juan S. Bonifacino ... [et al.]*, John Wiley & Sons, Inc.: 2006; pp 3.22.1-3.22.29.
42. Kormelink, T. G.; Arkesteijn, G. J.; Nauwelaers, F. A.; van den Engh, G.; Nolte-'t Hoen, E. N.; Wauben, M. H., Prerequisites for the analysis and sorting of extracellular vesicle subpopulations by high-resolution flow cytometry. *Cytometry. Part A : the journal of the International Society for Analytical Cytology* **2015**.